

PAPER • OPEN ACCESS

Patient Specific Diagnostics for cardiovascular diseases based on diagnostic imaging: an application to the aneurism of the ascending aorta

To cite this article: G. Querzoli *et al* 2019 *J. Phys.: Conf. Ser.* **1249** 012006

View the [article online](#) for updates and enhancements.



IOP | ebooks™

Bringing you innovative digital publishing with leading voices to create your essential collection of books in STEM research.

Start exploring the collection - download the first chapter of every title for free.

Patient Specific Diagnostics for cardiovascular diseases based on diagnostic imaging: an application to the aneurism of the ascending aorta

G. Querzoli^{1*}, V. Satta¹, G. Matta², S. Ferrari¹, M. G. Badas¹ and G. Bitti²

¹ DICAAR - University of Cagliari (Italy), Piazza d'Armi, Cagliari

² Department of Radiology - G. Brotzu Hospital, Cagliari (Italy)

*querzoli@unica.it

Abstract. In the framework of a collaboration between clinicians and engineers (namely, the Department of Radiology of the Brotzu Hospital in Cagliari and the group of experimental hydraulics at DICAAR - University of Cagliari), methodologies for the application of the in vitro study of the cardiovascular fluid mechanics to the support of the physical interpretation of the diagnostic imaging data are being tested. To this aim, we set up a mock-loop able to reproduce the physiologic pulsatile flow and designed to host a replica of aortic root made of transparent silicon rubber. Then, we developed a procedure to obtain a transparent and compliant replica of a patient specific ascending aorta from diagnostic images. The patient specific aorta model can be inserted in the mock-loop to study the fluid dynamics by means of particle image velocimetry techniques. We compared the flow in three cases, corresponding to physiological conditions, mild and severe aortic root dilation, observing significant differences in the redirection of the transvalvular jet and vortex evolution in the aortic flow. The observed fluid dynamics differences may have relevant implications on the thromboembolism and vascular tissue damage potential.

1. Motivation

The continuous development of the cardiovascular diagnostic imaging techniques yields, nowadays, the detailed volumetric information needed to perform accurate fluid-dynamic numerical simulations. On the other hand, the richer and richer information about the cardiovascular flows that can be gathered in vivo generates an increasing demand for physically based interpretation to translate imaging and in vivo flow data into diagnostically useful information. Patient specific modelling of the cardiovascular fluid mechanics aims addressing this issue. This kind of simulations was previously mostly performed by numerical methods [1,2].

At the same time, in vitro and in silico studies were performed aimed at getting insight on the fluid dynamics in the cardiovascular system and, particularly, in the left ventricle and in the proximal aorta, in order to provide a conceptual framework useful to interpret data obtained in vivo. At first the studies were based on idealized geometries, both for numerical simulations [3] and for laboratory models [4], which investigated physiological and pathological conditions [5–8] and the consequences of prosthetic valve implantations [9,10].

However, the recent improvement of the additive manufacturing allows the development of accurate laboratory models derived from volumetric diagnostic imaging, which can be worthy for investigating



patient specific models in controlled conditions, also in the context of aortic flows [11], where several issues deserve a deep insight.

Actually, today diagnostic imaging (e.g. 4D Cardiac Magnetic Resonance) gives comprehensive information about geometry of vessels and the characteristics of the aortic flow. Nonetheless, despite the fact that fluid dynamics is acknowledged to be the key element dictating the form and function of the heart and blood vessels, the onset of lesions or pathological forms and their evolution [12], clinical criteria determining the decision for a vascular intervention in presence of aneurisms are generally independent on fluid dynamic criteria and linked to simple geometrical conditions [13], for instance a threshold of the aneurism diameter, which can be not fully representative of the effective pathology risks.

In vitro studies of the aortic flow were developed at first using rigid aortic vessels (see, for instance, [14–16]), then flexible silicon rubber models, able to reproduce the physiological compliance of the aorta, were adopted ([5, 17–19]). Specifically, [5] reproduced quantitatively the aortic distensibility observed in vivo during the cardiac cycle, while [17] also simulated the flow within coronary arteries. However, these were all simulations on aortic vessels derived from mean geometric features corresponding to healthy or pathological conditions. To the best of the authors' knowledge, the only in vitro simulations performed on patient specific aortic root models were developed in order to investigate transcatheter aortic valve replacement (TAVR) performance [20] or to investigate TAVR hemodynamic consequences in case of different sinus morphologies [21], while only one paper [22] is focused on investigating flow patterns in the ascending aorta in case of two patient specific models: MRI and 3D-PTV were applied to the whole aortic arch excluding Valsalva sinus and without any upstream aortic valve to two models reproducing physiological and aneurysmal conditions. Results showed how high turbulence intensity and pressure loss are measured in the diseased aorta with respect to the healthy geometry.

In the framework of a collaboration between the Department of Radiology at the Brotzu Hospital (Cagliari, Italy) and the group of experimental hydraulics at DICAAR (University of Cagliari), the experimentation and use of new techniques for the in-vitro simulation of the fluid dynamics of the proximal aorta in patient specific models is currently being tested. A procedure to obtain a transparent and compliant replica of a patient specific ascending aorta from diagnostic images was developed and the aorta phantoms can be inserted in a mock-loop, able to reproduce the physiologic pulsatile flow, and optical velocimetry techniques are used to obtain a time-resolved evolution of the velocity field.

The present study is focused on the comparison of flow in patient specific ascending aortas with aneurisms of different sizes, in presence of a bileaflet aortic valve. The analysis on the mean and turbulent velocity fields reveal how the different morphology substantially affects the transvalvular jet redirection and the vortex evolution during the cardiac cycle.

2. Methods

The methods developed in order to infer diagnostic information from a patient specific in-vitro model consists in three main steps, which are detailed in the following.

2.1. Geometry model set-up

The aorta models are based on the diagnostic images acquired by the clinicians by means of a contrast-enhanced CT angiography, using tomographic sections 0.6 mm in depth (Fig. 1). Raw anonymized data were subject to a segmentation procedure in order to identify the lumen of the vessels (Fig. 2). Specifically, the aorta lumen was selected and a series of sections orthogonal to the vessel axis were traced (Fig. 3). Since the experimental apparatus at present is not yet ready to host a model reproducing the aortic curvature, the obtained aortic sections were then aligned on a rectilinear axis, and a filtering procedure aimed at getting rid of the segmentation artifacts was applied. Namely, the ascending aorta is almost symmetric about its plane of curvature, whose axis was considered to rectify the model. Bileaflets valves may in general be implanted in different positions [23,24], which have an impact on the flow development and specifically influence the dynamics of the sinus vortex at the end

of systole [25]. Here, the valve plane of symmetry, i.e. the one parallel to the two open leaflets, is perpendicular to the ascending aorta's plane of curvature, hence the leaflet open inside the sinus corresponding to the left coronary artery position.

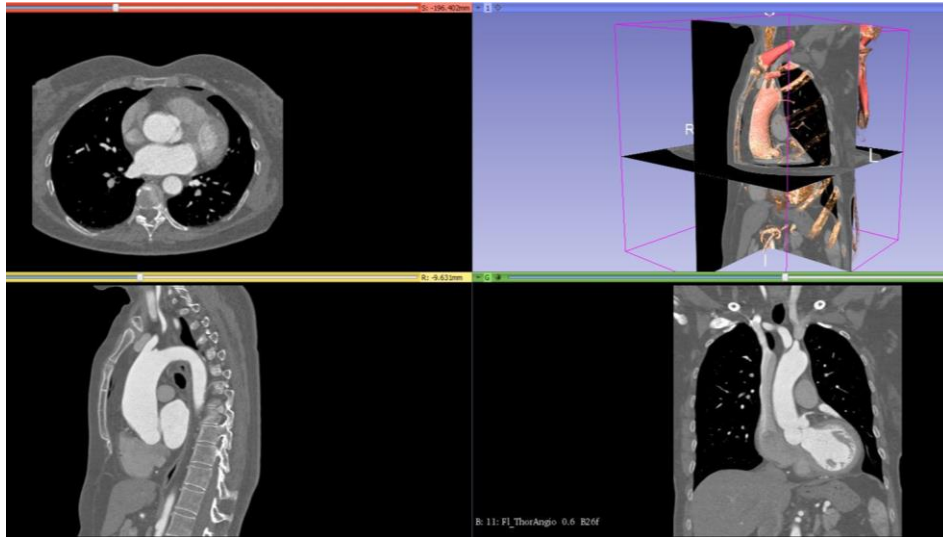


Figure 1. Example of CT diagnostic images.

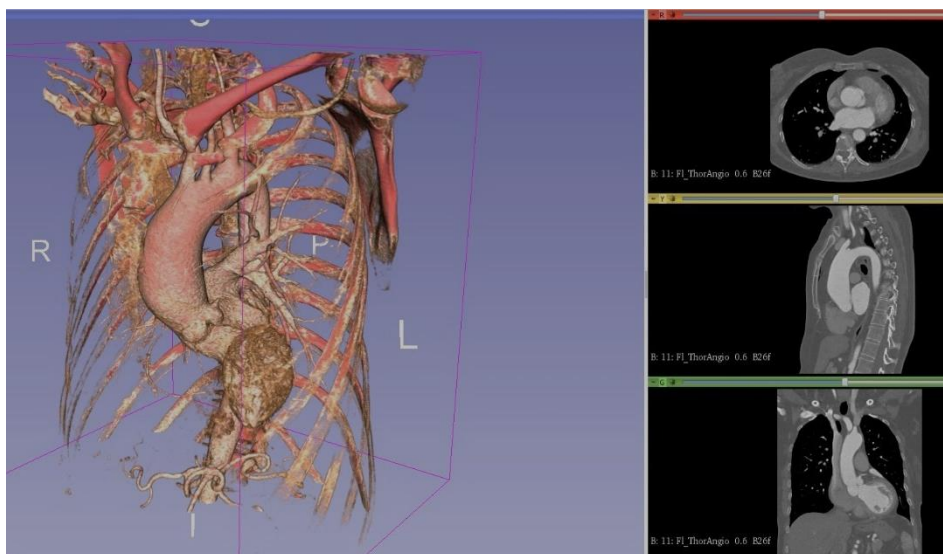


Figure 2. Segmentation procedure to identify the vessel lumen.

2.2. Transparent model realization

The geometric model was then 3D printed, and it was manually smoothed to obtain a regular and even surface, useful to produce a silicon rubber model following the procedure better detailed in [5] (Fig4). Specifically, in the present study, three degrees of aortic root dilation were compared: the first one corresponds to a healthy one and is 28 mm in diameter (Fig. 5a), the second one, whose diameter is 48 mm, is just below the clinical threshold for an intervention (Fig. 5b) and the third one corresponds to a severe root dilation, 64 mm in root diameter (Fig. 5c).

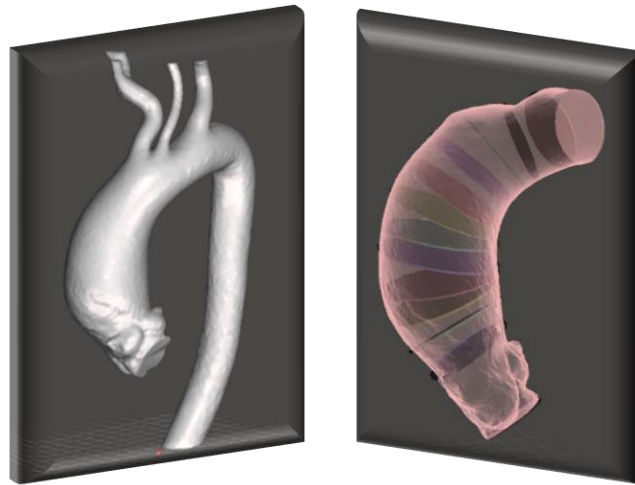


Figure 3. Segmentation of the aorta (left panel) and identification of normal sections (right panel).

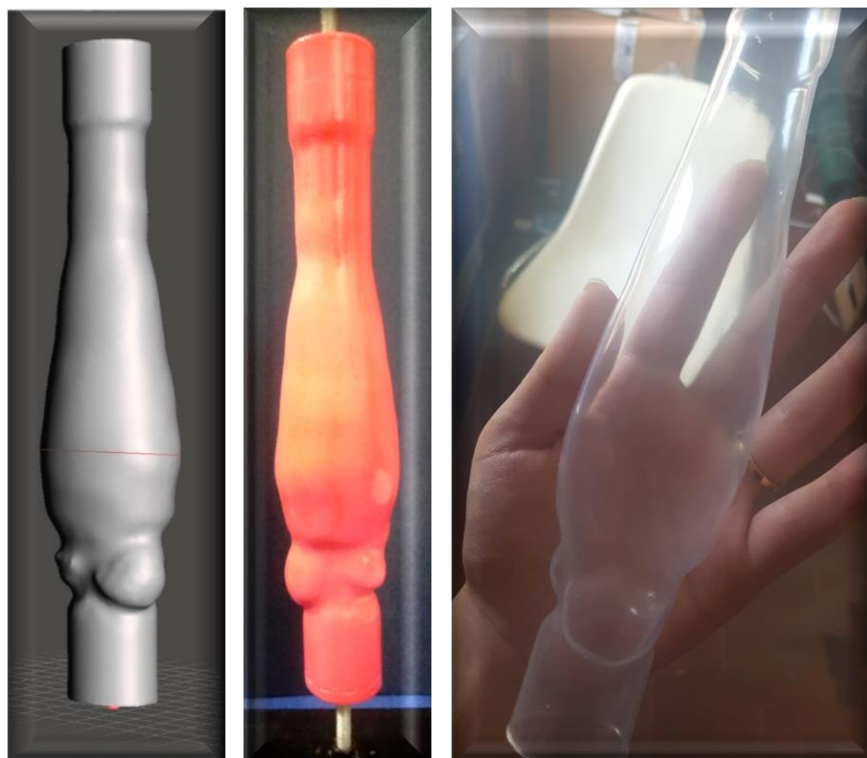


Figure 4. Procedure to go from the rectified geometry (left panel) to the 3D printed one (central panel), up to the transparent silicon rubber one (right panel).



Figure 5. 3D printed models of the three analysed cases: healthy case (28 mm in diameter, top panel), mild dilation (48 mm in diameter, central panel), severe dilation (64 mm in diameter, bottom panel).

2.3. Simulation in the pulse duplicator

The pulse duplicator (Fig. 6) able to reproduce the physiological flow rate from the left ventricle and entering the aortic vessel is similar to the one adopted in [4–6]. A linear motor, controlled in velocity by a personal computer, moves according to a prescribed speed law, hence determining a periodic volume change of the ventricular chamber and, consequently, a flow entering the aortic root towards a bileaflet mechanical valve (Sorin Bicarbon), whose closure avoids the flow regurgitation during the systolic phase. A one-way valve is placed at the end of the aortic vessel, which is inside a 20-mm-thick Plexiglass tank. The impedance of the circulatory system is reproduced tuning adjustable head losses and a compliance chamber inserted along the conduits.

Since the model geometric scale is 1:1 but the working fluid, water, has a viscosity that is roughly 1/3 of the blood's one, in order to maintain the dynamic similarity, simulations were performed multiplying the physiological cardiac period for three times. This allows matching the Womersley and Reynolds number between experiments and real case:

$$Wo = \sqrt{\left(\frac{D^2}{\nu T}\right)}; \quad Re = \frac{UD}{\nu} \quad (1)$$

where D is the aortic diameter, ν is the kinematic viscosity, T the cardiac period, and U the peak velocity through the aortic valve. A physiological inlet transvalvular flow curve was reproduced, corresponding to a stroke volume of 64 ml and 70 beats per second, and it was applied for the three simulated geometries. A light sheet illuminates the axial symmetry plane of the vessel, where a high velocity camera records 585 frames per second with a resolution of 896×1120 pixel. The working fluid is water, and pine pollen particles (20 μm of mean diameter) are dispersed within the fluid for velocity measurements. Acquired images are then analyzed by means of feature tracking velocimetry (FTV), an in-house two-frame particle tracking velocimetry, which was proven to be robust to high velocity gradients and seeding density variations [26–28].

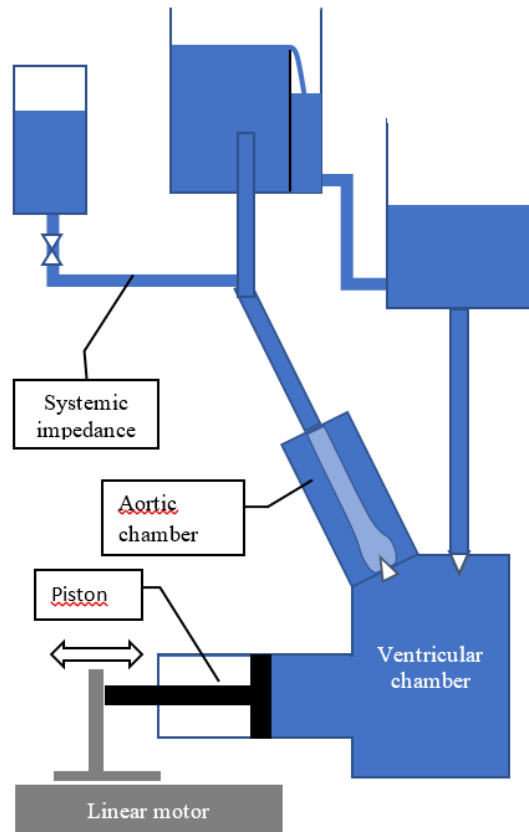


Figure 6. Sketch of the pulse duplicator.

The main steps of this technique are: for each frame couple, regions with high intensity gradients are identified by means of the Harris detector; interrogation windows centered on features identified in the first frame are compared with shifted windows in the second frame corresponding to a range of possible displacements; the displacement minimizing windows dissimilarity is determined by means of the Lorentzian estimator; velocity are then computed dividing for each feature, the displacement by the time interval between frames.

For each aortic geometry, more than 120'000 velocity fields were measured, corresponding to 90 heart cycles. Obtained samples were then mapped on a regular grid and in phase averages were performed to obtain the mean flow field time evolution.

3. Results

Figure 7 displays the color maps of the velocity magnitude, made non-dimensional by peak velocity, U , and corresponding streamlines for the three simulations and three characteristic instants of the flow: the systolic peak ($t/T=0.07$), decelerating ejection ($t/T = 0.10$) and the systole end ($t/T = 0.21$). The plots highlight the multijet flow generated by the bileaflet valve for all the geometries. However the jets evolution is quite different for the three cases: in the healthy case the three jets evolve almost simultaneously, the two lateral ones being squeezed on the lateral walls, and they rapidly reach the distal region; in case of aneurysm, especially for the severe one, the lateral jets expand and they remain confined in the sinus area highlighting large and persistent rotational regions occur in the systolic phase

Turbulent kinetic energy (TKE) color maps made non-dimensional by peak velocity, U^2 , are displayed in Figure 8 for the same characteristic instants plotted in Figure 7, and they show high TKE levels at

the leading border of the three jets for all the three simulations, with the different time evolution already highlighted in velocity colormaps. Temporal average of TKE fields was also performed in order to infer a global information during the cardiac cycle (Figure 9). Comparing the three cases, a different picture emerges: in the healthy aorta the turbulence is confined in the root, while in the 48mm aorta higher turbulence level is observed in the central transvalvular jet and in the 64mm aorta most of the turbulence is confined in the distal portion of the root. A sudden expansion in the aortic section, especially in the severe aortic dilation, causes a flow separation, which enhances turbulence and pressure loss, and may eventually cause aneurysm growth or vessel rupture.

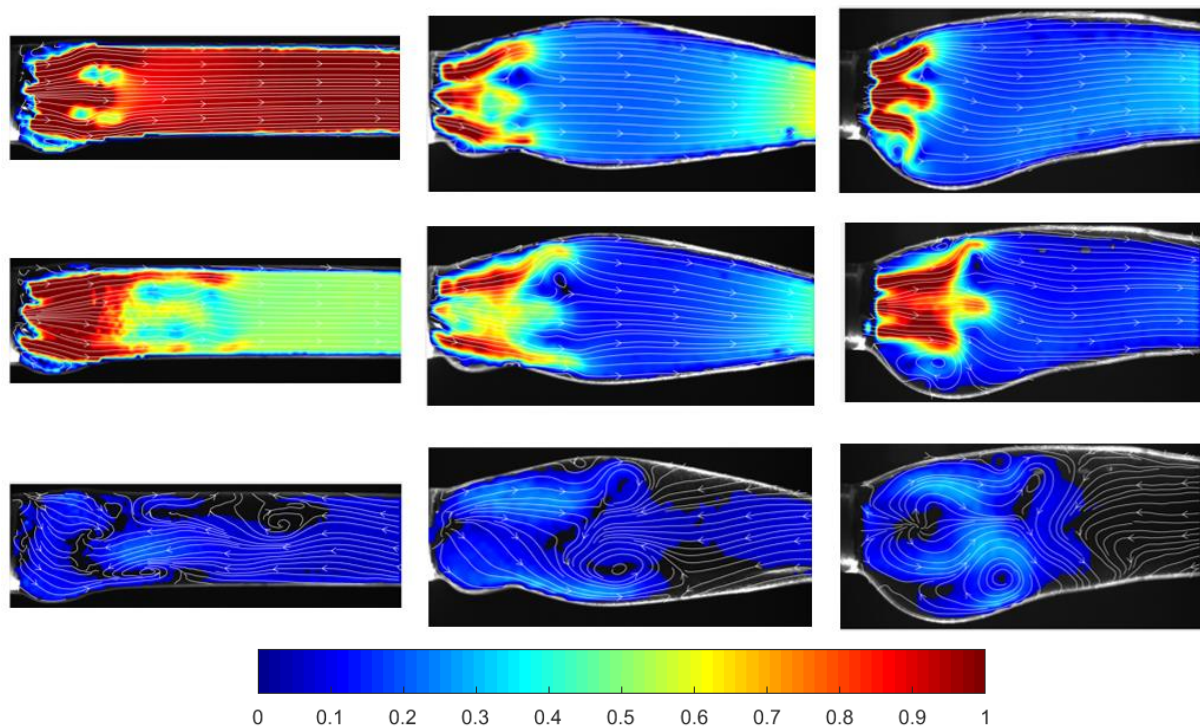


Figure 7. Velocity colormaps made non-dimensional by the peak velocity U computed for the healthy case (left column), mild dilation (central column) and severe dilation (left column) at different instants of the cycle the systolic peak ($t/T=0.07$ – first row), during decelerating ejection ($t/T = 0.10$ – second row) and at the systole end ($t/T = 0.21$ – third row). Streamlines are superimposed as white lines.

4. Discussion and future development

An in vitro analysis of the flow in three patient specific models of ascending aorta is presented. Simulated cases correspond to healthy condition, mild and severe aortic dilation. Optical measurements were used to study mean and turbulent flow field evolution during the cardiac cycle, and relevant differences among the three cases.

Although the velocity fields were acquired on a symmetry aortic plane, the two dimensional measurements do not allow to fully capture the three dimensional flow around the sinus region. Actually, due to the rectification of the model and the absence of the aortic arch, the flow is representative of real conditions only in the first part of the aortic root, where the aortic curvature plays a negligible effect. Moreover, although the aortic vessels reproduce the in-vivo elasticity, all the models have similar and homogeneous mechanic properties, while important changes in elastic modulus may affect aneurismatic vessels and the aortic wall properties are characterized from tissue inhomogeneities, which cannot be reproduced in the model.

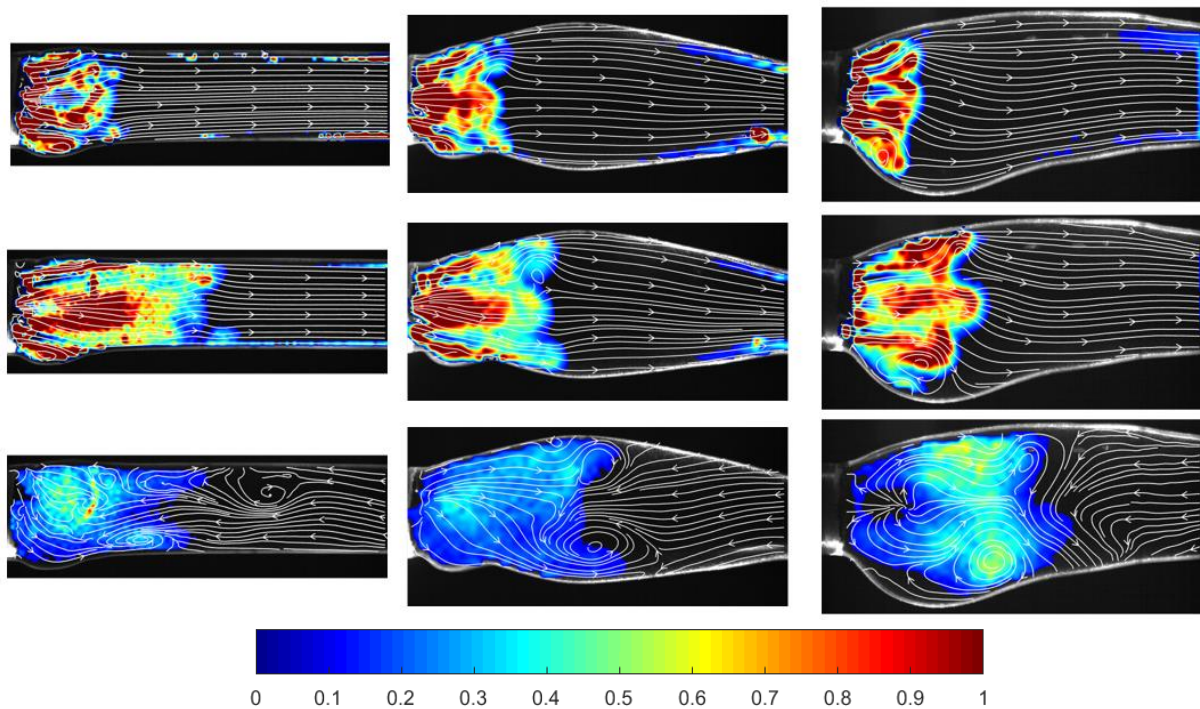


Figure 8. Turbulent kinetic energy (TKE) colormaps, made non-dimensional by peak velocity, U^2 , computed for the healthy case (left column), mild dilation (central column) and severe dilation (left column) at different instants of the cycle the systolic peak ($t/T=0.07$ – first row), during decelerating ejection ($t/T = 0.10$ – second row) and at the systole end ($t/T = 0.21$ – third row). Streamlines are superimposed as white lines.

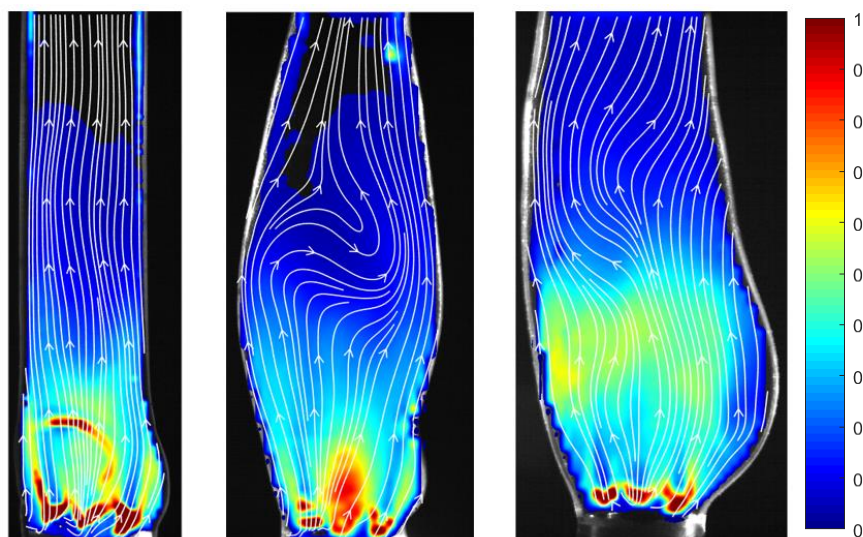


Figure 9. Turbulent kinetic energy (TKE) colormaps, made non-dimensional by peak velocity, U^2 , averaged during the whole cardiac cycle for the healthy case (left column), mild dilation (central column) and severe dilation (left column).

However, despite its limitations, this work represents a valuable contribution demonstrating how in vitro studies, getting insights on the patient specific fluid dynamics, may provide the clinicians

relevant information for the interpretation of the diagnostic images. In fact, present measurements allow characterizing the flow patterns and their evolution as well as turbulent phenomena developing in the patient specific aortic roots, and they highlight significant differences in the redirection of the transvalvular jet and vortex evolution in the aortic flow.

Indeed, physiological inflow conditions are not reproduced in the aortic model, since a mechanical bileaflet valve is placed upstream. Hence, the obtained flow is representative only in cases of a mitral valve replacement. However, in case an aortic valve replacement is needed, understanding the possible interaction of prosthetic valve with aortic vessel is fundamental since it can contribute to predict aortic remodeling and, in case different valves are compared, simulations may provide relevant information to the clinicians. Specifically, bileaflet valves, which are still widely due to their long-term durability, are responsible for a non-physiological hemodynamics, which may lead to several complications (aortic stenosis, platelet activation, blood clots [24]), but these effects may be quite different according to the patient specific geometry they are implanted on.

The collaboration between clinicians and engineers is going on and the adoption of a physiological valve as well as the development of a new set-up able to host the entire aortic arch is currently under study. The fulfilment of these tasks would provide a step forward to obtaining more realistic and clinically meaningful information from in vitro simulations.

Acknowledgments

The authors are grateful to Antonio Mascia for his valuable contribution in building the experimental set-up. This work is part of the project “PSD for Cardiovascular Diseases (Patient Specific Diagnostics for Cardiovascular Diseases)”, funded by the Sardinian Regional Government through the Public Procedure “Promozione di nuovi mercati per l’innovazione nella PA” under the POR FESR Sardegna 2014/2020.

References

- [1] Fedele M, Faggiano E, Dedè L and Quarteroni A 2017 A patient-specific aortic valve model based on moving resistive immersed implicit surfaces *Biomechanics and Modeling in Mechanobiology* **16** 1779–803
- [2] Celotto C, Zovatto L, Collià D and Pedrizzetti G 2019 Influence of mitral valve elasticity on flow development in the left ventricle *European Journal of Mechanics - B/Fluids* **75** 110–8
- [3] Domenichini F and Pedrizzetti G 2011 Intraventricular vortex flow changes in the infarcted left ventricle: numerical results in an idealised 3D shape *Computer Methods in Biomechanics and Biomedical Engineering* **14** 95–101
- [4] Cenedese A, Del Prete Z, Miozzi M and Querzoli G 2005 A laboratory investigation of the flow in the left ventricle of a human heart with prosthetic, tilting-disk valves *Experiments in Fluids* **39** 322–35
- [5] Querzoli G, Fortini S, Espa S, Costantini M and Sorgini F 2014 Fluid dynamics of aortic root dilation in Marfan syndrome *Journal of Biomechanics* **47** 3120–8
- [6] Badas M G, Espa S, Fortini S and Querzoli G 2015 3D Finite Time Lyapunov Exponents in a left ventricle laboratory model EPJ Web of Conferences vol 92
- [7] Badas M G, Domenichini F and Querzoli G 2017 Quantification of the blood mixing in the left ventricle using Finite Time Lyapunov Exponents *Meccanica* **52** 529–44

- [8] Di Labbio G, Vétel J and Kadem L 2018 Material transport in the left ventricle with aortic valve regurgitation *Physical Review Fluids* **3**
- [9] Wang J, Gao Q, Wei R and Wang J 2017 Experimental study on the effect of an artificial cardiac valve on the left ventricular flow *Experiments in Fluids* **58**
- [10] Querzoli G, Fortini S and Cenedese A 2010 Effect of the prosthetic mitral valve on vortex dynamics and turbulence of the left ventricular flow *Physics of Fluids* **22** 041901
- [11] Yazdi S G, Geoghegan P H, Docherty P D, Jermy M and Khanafer A 2018 A Review of Arterial Phantom Fabrication Methods for Flow Measurement Using PIV Techniques *Annals of Biomedical Engineering* **46** 1697–721
- [12] Richter Y and Edelman E R 2006 Cardiology Is Flow *Circulation* **113** 2679–82
- [13] Erbel et al 2014 ESC Guidelines on the diagnosis and treatment of aortic diseases: Document covering acute and chronic aortic diseases of the thoracic and abdominal aorta of the adult The Task Force for the Diagnosis and Treatment of Aortic Diseases of the European Society of Cardiology (ESC) *European Heart Journal* **35** 2873–926
- [14] Bellhouse B J and Talbot L 1969 The fluid mechanics of the aortic valve *Journal of Fluid Mechanics* **35** 721
- [15] Grigioni M, Daniele C, D’Avenio G and Barbaro V 2001 The influence of the leaflets’ curvature on the flow field in two bileaflet prosthetic heart valves *Journal of Biomechanics* **34** 613–21
- [16] Balducci A, Grigioni M, Querzoli G, Romano G P, Daniele C, D’Avenio G and Barbaro V 2004 Investigation of the flow field downstream of an artificial heart valve by means of PIV and PTV *Experiments in Fluids* **36** 204–13
- [17] Querzoli G, Fortini S, Espa S and Melchionna S 2016 A laboratory model of the aortic root flow including the coronary arteries *Experiments in Fluids* **57**
- [18] Linde T, Hamilton K F, Navalon E C, Schmitz-Rode T and Steinseifer U 2012 Aortic Root Compliance Influences Hemolysis in Mechanical Heart Valve Prostheses: An In-Vitro Study: *The International Journal of Artificial Organs*
- [19] Gülan U, Lüthi B, Holzner M, Liberzon A, Tsinober A and Kinzelbach W 2012 Experimental study of aortic flow in the ascending aorta via Particle Tracking Velocimetry *Experiments in Fluids* **53** 1469–85
- [20] Rotman O M, Kovarovic B, Chiu W-C, Bianchi M, Marom G, Slepian M J and Bluestein D 2019 Novel Polymeric Valve for Transcatheter Aortic Valve Replacement Applications: In Vitro Hemodynamic Study *Annals of Biomedical Engineering* **47** 113–25
- [21] Hatoum H, Dollery J, Lilly S M, Crestanello J and Dasi L P 2019 Impact of patient-specific morphologies on sinus flow stasis in transcatheter aortic valve replacement: An in vitro study *The Journal of Thoracic and Cardiovascular Surgery* **157** 540–9
- [22] Gülan U, Calen C, Duru F and Holzner M 2018 Blood flow patterns and pressure loss in the ascending aorta: A comparative study on physiological and aneurysmal conditions *Journal of Biomechanics* **76** 152–9

- [23] Gülan U and Holzner M 2018 The influence of bileaflet prosthetic aortic valve orientation on the blood flow patterns in the ascending aorta *Medical Engineering & Physics* **60** 61–9
- [24] Sotiropoulos F, Le T B and Gilmanov A 2016 Fluid Mechanics of Heart Valves and Their Replacements *Annual Review of Fluid Mechanics* **48** 259–83
- [25] De Tullio M D, Cristallo A, Balaras E and Verzicco R 2009 Direct numerical simulation of the pulsatile flow through an aortic bileaflet mechanical heart valve *Journal of Fluid Mechanics* **622** 259
- [26] Besalduch L A, Badas M G, Ferrari S and Querzoli G 2013 Experimental Studies for the characterization of the mixing processes in negative buoyant jets *EPJ Web of Conferences* **45** 01012
- [27] Besalduch L A, Badas M G, Ferrari S and Querzoli G 2014 On the near field behavior of inclined negatively buoyant jets *EPJ Web of Conferences* **67** 02007
- [28] Garau M, Badas M G, Ferrari S, Seoni A and Querzoli G 2018 Turbulence and Air Exchange in a Two-Dimensional Urban Street Canyon Between Gable Roof Buildings *Boundary-Layer Meteorology* **167** 123–43